

DEPARTMENT OF THE INTERIOR

U.S. GEOLOGICAL SURVEY

In-Situ Stress Project,

Technical Report Number 5:

Interpretation of Hydraulic Fracturing Data from  
Xiaguan, western Yunnan, China

by

Zoback, M.D.<sup>1,2</sup>, Springer, J.E.<sup>1</sup>, Zhai Qingshan<sup>3</sup>,  
Haimson, B.C.<sup>4</sup>, Lee, M.Y.<sup>4</sup>, and Li Fangquan<sup>3</sup>

U.S. Geological Survey

Open-File Report 87-476

Prepared in cooperation with the State Seismological Bureau of China, the University of Wisconsin, and Stanford University.

This report is preliminary and has not been reviewed for conformity with U.S. Geological Survey editorial standards and stratigraphic nomenclature. Any use of trade names is for descriptive purposes only and does not imply endorsement by the USGS.

<sup>1</sup>  
USGS  
Menlo Park, CA

<sup>2</sup>  
Stanford University  
Stanford, CA

<sup>3</sup>  
Institute of Crustal Dynamics  
Beijing, China

<sup>4</sup>  
University of Wisconsin  
Madison, WI

1987

## CONTENTS

	Page
Abstract	1
Introduction	1
Methods	3
Determination of Shmin	6
Results	9
<u>Test A - 85 m</u>	11
<u>Test B - 198 m</u>	13
<u>Test C - 214 m</u>	13
<u>Test D - 233 m</u>	13
<u>Test E - 250 m</u>	13
<u>Test F - 419 m</u>	18
<u>Test G - 452 m</u>	18
Discussion	18
Conclusions	21
References	23
Appendix	26

## FIGURES

Figure 1: Location map of the western Yunnan region where the stress measurements were made.	2
Figure 2: Generalized fault map showing the location of the hole. Faults keyed by number on the map are: 1: Red River fault, 2: Madeng fault, 3: Lancang River fault, 4: Chenghai-Binchuan fault, 5: Heqing-Eryuan fault, 6: Lijiang fault, 7: Jianchuan fault, and 8: Zhongdian fault. For more information on the faults, see Springer et al. (1987b).	4
Figure 3: Example of a pressure-time record showing the ISIP, Pr, and Pb.	5
Figure 4: Example of the tangent method of choosing an inflection point on a pressure-time record.	7

	Page
Figure 5: Example showing the semilog method of choosing the ISIP. After Haimson and Lee (1984).	8
Figure 6: Example of the negative exponential non-linear regression method for choosing the ISIP (after Haimson and Lee, 1987).	10
Figure 7: Example of the flow-rate vs pressure method for choosing the ISIP.	10
Figure 8: Tracing of the impression packer from Test A.	12
Figure 9: Tracing of the impression packer from Test B.	14
Figure 10: Tracing of the impression packer from Test C.	15
Figure 11: Tracing of the impression packer from Test D.	16
Figure 12: Tracing of the impression packer from Test E.	17
Figure 13: Tracing of the impression packer from Test F.	19
Figure 14: Tracing of the impression packer from Test G.	20
Figure 15: Plot of $S_{hmin}$ , $S_{Hmax}$ , $S_v$ , and $P_o$ vs depth. The envelope of frictional failure in a thrust faulting mode is shown for frictional coefficient values of 0.6 to 1.0 using the relationship derived by Zoback and Healy (1984).	22

#### TABLES

Table 1: General data on the Xiaguan borehole.	11
Table 2: Stress determinations from Xiaguan.	11

INTERPRETATION OF HYDRAULIC FRACTURING DATA FROM XIAGUAN,  
WESTERN YUNNAN, CHINA

M.D. Zoback, J.E. Springer, Zhai Qingshan, B.C. Haimson,  
M.Y. Lee, and Li Fangquan

---

ABSTRACT

Hydraulic fracturing stress measurements were performed in a 500 m-deep well at Xiaguan in western Yunnan, a region of high seismicity and active normal and strike-slip faulting. The well penetrated Ordovician clastic sediments and older Ultramafic intrusives. Five methods were used to determine the instantaneous shut-in pressure. These were: 1. the inflection point method (IP), 2. the semilog method (SL), 3. a nonlinear regression method for isolating the negative exponential part of the decay curve (NLR), 4. minimal flow-rate pumping pressure (LF), and 5. flow-rate vs pressure (FR). These methods were compared and upper and lower bounds were placed on the value of  $S_{hmin}$ . The criterion for choosing or rejecting a method was its internal consistency and its consistency compared to other methods. The two most successful methods were the inflection point method, which is the most subjective and the nonlinear regression method which is relatively objective. The semilog method did not provide useable results in these tests.

Impressions run after the tests provided evidence that vertical hydraulic fractures had been created, although inclined fractures were usually visible on the pre-hydrofrac televiewer log. Because of poorly controlled pumping rates, fracture reopening pressures were hard to pick accurately and are presented as ranges of possible values. These ranges yielded uncertainties for the value of the maximum horizontal stress that varied from 10% up to 36%.

The magnitude of  $S_{hmin}$  in the Xiaguan hole is consistently close to, but slightly higher than the vertical stress inferred from the average rock density. This is close to the transition between a thrust faulting and strike-slip stress regime. Analysis of the maximum shear stress using reasonable values for the coefficient of friction suggests that the rocks are not close to failure in these modes. Considering that the well is only 500 m deep, these stress magnitudes do not contradict the observed strike-slip to normal tectonic style of the region. Orientations of hydraulic fractures from the well are consistent with a N-S to NNE-SSW maximum horizontal stress of direction.

INTRODUCTION

The joint Sino-U.S. in-situ stress program was undertaken in an effort to understand the tectonic stress field in a seismically active area of northwestern Yunnan, China (fig. 1). The hydraulic fracturing method was chosen because of the

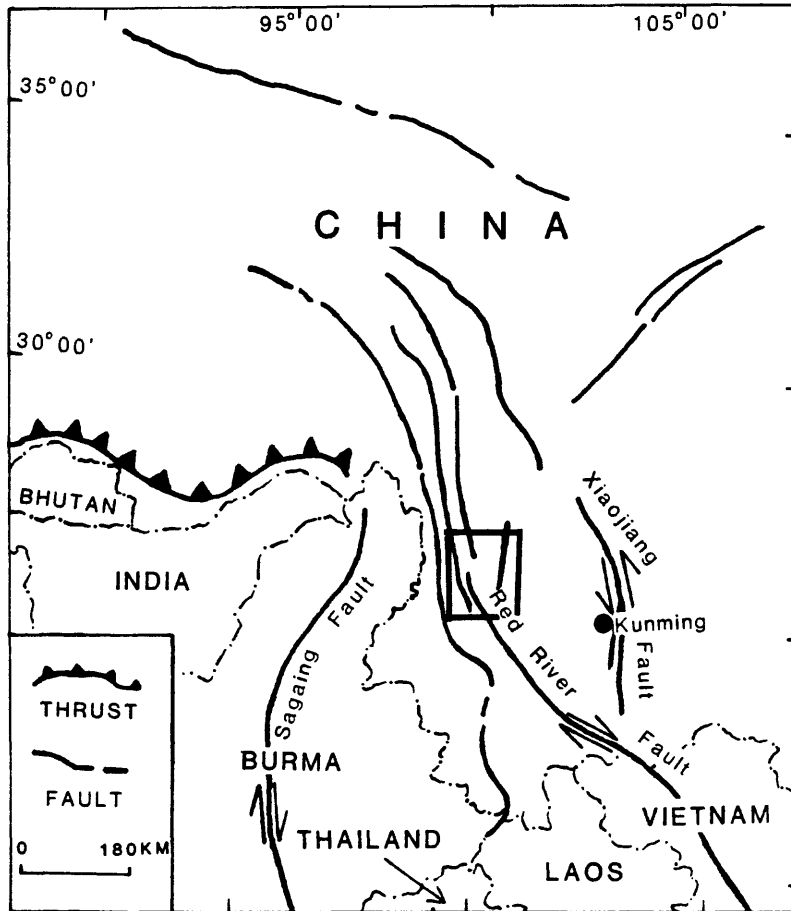


Fig. 1. Location map showing the northern Yunnan region where the stress measurements were made. The rectangle represents the area of fig. 2.

advantage of being able to make deep measurements (Haimson and Fairhurst, 1970). The first set of measurements was performed in a 500 m-deep well at Xiaguan (fig. 2). The well was drilled in the northern segment of the Red River fault zone and the measurements there were carried out in 1983.

The region is characterized by active normal and strike-slip faulting (Allen et al., 1984; Liu et al., 1986). The most prominent tectonic feature is the Red River fault which has a length of at least 900 km and shows both normal and right-lateral strike-slip movement. Another set of faults trends northeast and these have normal and left-lateral motion on them (Li et al., 1986; Liu et al., 1986; Wu and Deng, 1985; Yan et al., 1983).

The Xiaguan well was drilled through Ordovician sandstones and shales to a depth of 414 m. Below that depth, older Ultramafic rocks were encountered. The bottom two tests were performed in the ultramafic rocks at depths of 419 m and 452 m. The rock was highly fractured throughout most of the well. The local geology and analysis of televiwer logs are described in an open-file report (Springer et al., 1987a). The analysis of the hydraulic fracturing stress measurements is presented in this paper. We first describe the methods used to interpret the data, then we present the results of each method and place upper and lower bounds on the principal stresses.

#### METHODS

Hubbert and Willis (1957) first described the relationship between hydraulic fracturing and in-situ stress. The method is based on the principle that, in mechanically isotropic rock, a hydraulically induced fracture will propagate in a plane normal to the least principal stress. Zoback and Zoback (1980) and McGarr and Gay (1978) present data supporting the assumption that, at depth, the vertical stress  $S_v$  and the maximum and minimum horizontal stresses ( $S_{Hmax}$  and  $S_{Hmin}$ ) are nearly parallel to the three principal stresses.

The hydraulic fracturing technique consists of isolating a section of the borehole with inflatable rubber packers and pressurizing the interval between them. Assuming that the rock behaves elastically, the minimum tangential compressive stress occurs along the azimuth of  $S_{Hmax}$  and enough applied pressure results in tensile failure of the well bore in this direction. The induced fracture is usually vertical. An example of a pressure-time record is shown in fig. 3. The pressure at which the rock breaks, indicated by the first peak in the pressure-time record, is called the breakdown pressure,  $P_b$ . After the breakdown pressure is reached, the well is shut in and the pressure decays rapidly. When the fracture closes, the rate of this decay changes. The pressure at which this happens is called the instantaneous shut-in pressure (ISIP). Because this is the minimum pressure required to hold the fracture open, it is considered to be equal to the least horizontal principal stress.

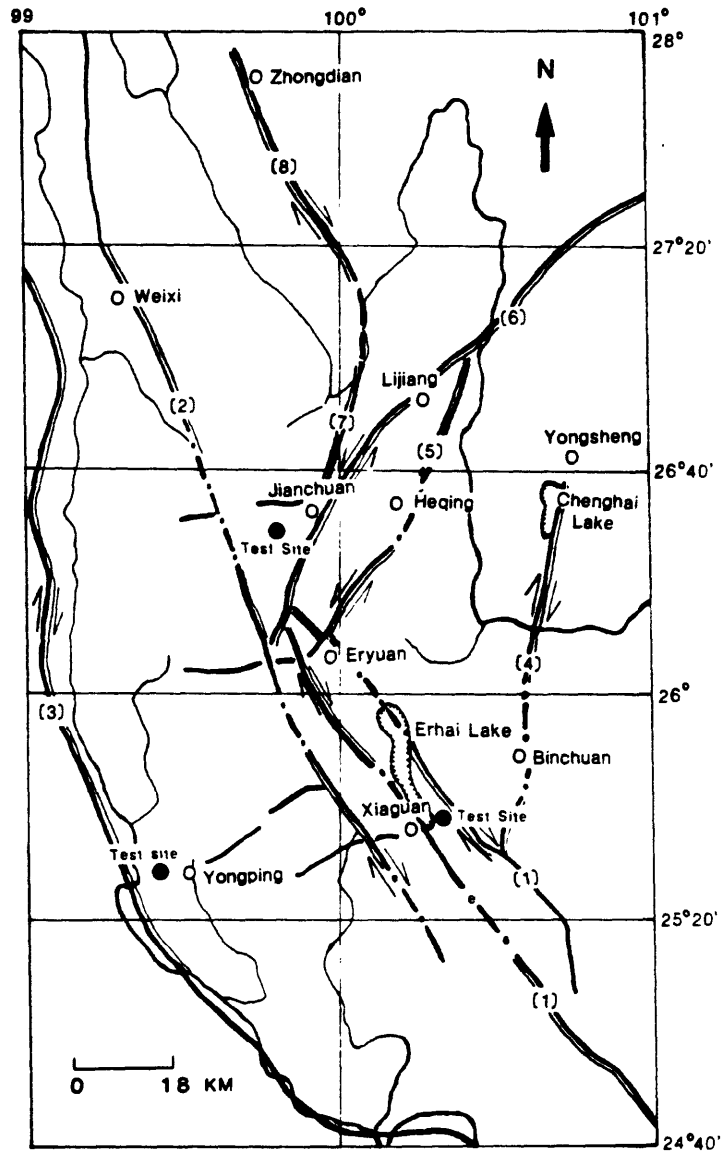


Fig. 2. Generalized fault map showing the location of the hole. Faults keyed by number on the map are 1. Red River fault, 2: Madeng fault, 3: Lancang River fault, 4: Chenghai-Binchuan fault, 5: Heqing-Eryuan fault, 6: Lijiang fault, 7: Jianchuan fault, and 8: Zhongdian fault. For more information on the faults, see Springer et al. (1987b).

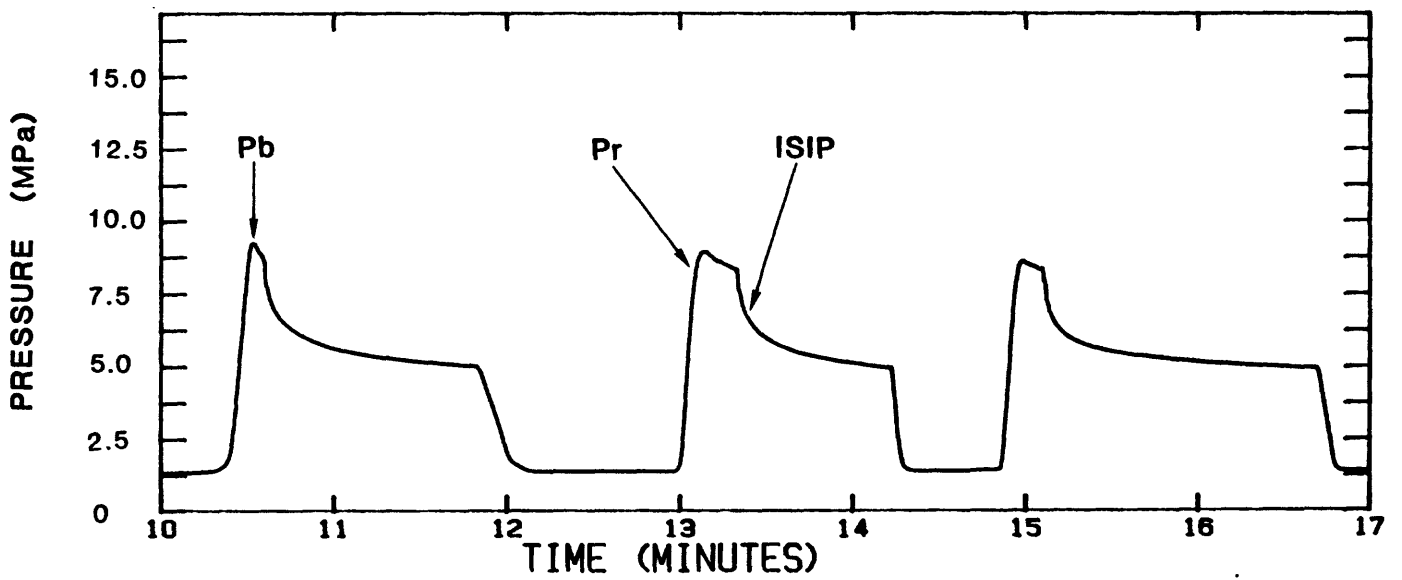


Fig. 3. Example of a pressure-time record showing the ISIP, Pr, and Pb.

Using the Kirsch equations (Jaeger and Cook, 1976) for stress concentrations around the borehole, Haimson and Fairhurst (1967) derived the relationship between  $P_b$ ,  $SH_{max}$ ,  $SH_{min}$ , the pore pressure  $P_o$  and the tensile strength,  $T$ :

$$P_b = 3SH_{min} - SH_{max} - P_o + T \quad [1]$$

Since data on the tensile strength were not available, the fracture reopening pressure  $P_r$  was used to determine  $SH_{max}$ . This is equivalent to a breakdown pressure with zero tensile strength and is related to  $SH_{max}$  by the following relationship (Bredehoeft et al., 1976):

$$P_r = 3SH_{min} - SH_{max} - P_o \quad [2]$$

The fracture reopening pressure is estimated from a change in the pressure buildup curve during a pumping cycle (fig. 3). Constant flow rates yield the best estimates of  $P_r$  and the best picks for  $P_r$  typically come from the third pumping cycle (Hickman and Zoback, 1983). Because we were unable to control the rates as well as we would have liked, the values of  $P_r$  were usually ambiguous and we picked them from whatever cycles we could. We present estimates of  $P_r$  values as upper and lower bounds.

#### Determination of $SH_{min}$

Because the ISIP on the decay curve is not always visible by inspection, several different methods were used to determine the value of  $SH_{min}$ . These methods can be divided into two categories, those involving the decay curve and those involving pumping pressures. The methods involving the decay curve are the inflection point method (IP), semilog method (SL), and nonlinear regression (NLR). The methods involving pumping pressures are; flow rate vs pressure (FR) and low flow rate pumping pressure (PLR). These methods are briefly described below:

Inflection Point Method. The inflection point method is the simplest method and it involves picking the inflection point on the decay curve after shut in. When the inflection point is not visible by inspection, a variation on this method, was used successfully by Gronseth and Kry (1983) in high modulus crystalline rock. To use this method, a straight line is drawn tangent to the decay curve from the point of shut in (fig. 4). The point at which this line departs from the decay curve is taken to be the ISIP.

The Semilog Method. In some of the Xiaguan tests, a semilog method was attempted. Aamodt and Kuriagawa (1983) proposed a method based on plotting the log of the pressure decay against linear time. We use a simpler method, used by Haimson and Lee (1984), in which linear pressure is plotted against log time. With this method, the decay curve takes on a steep linear character and, at the ISIP, the slope makes an abrupt change (fig. 5).

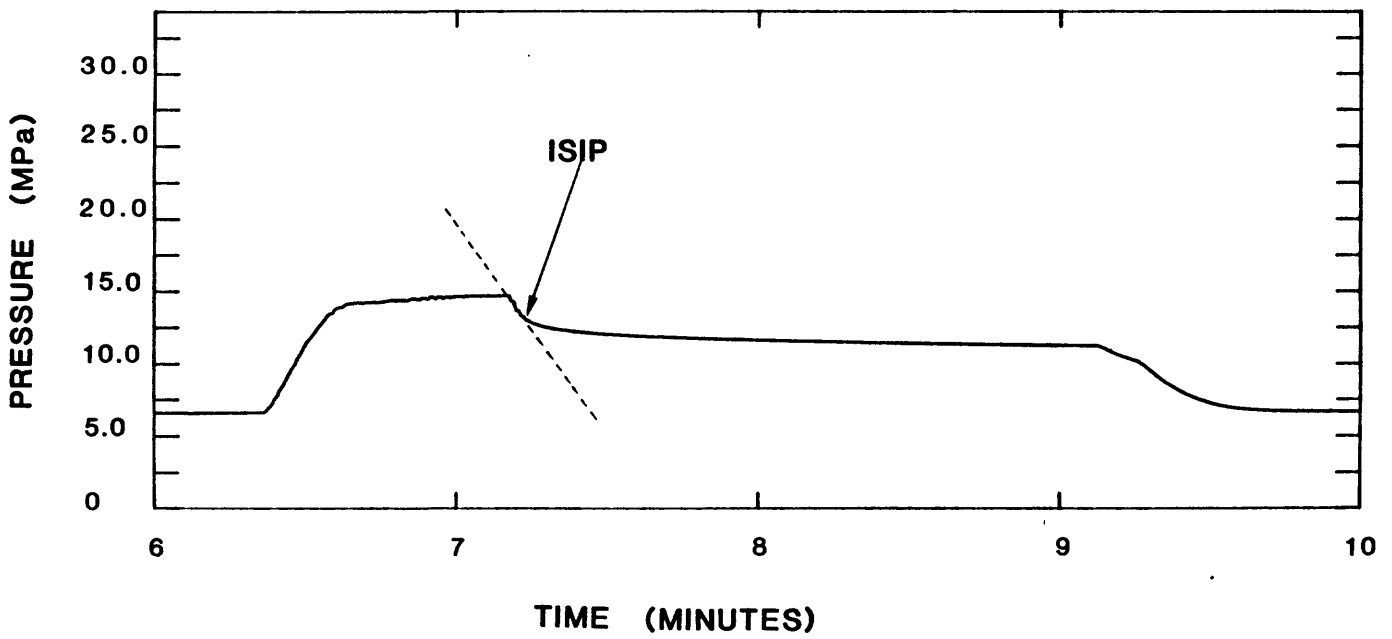


Fig. 4. Example of the tangent method of choosing an inflection point on a pressure-time record.

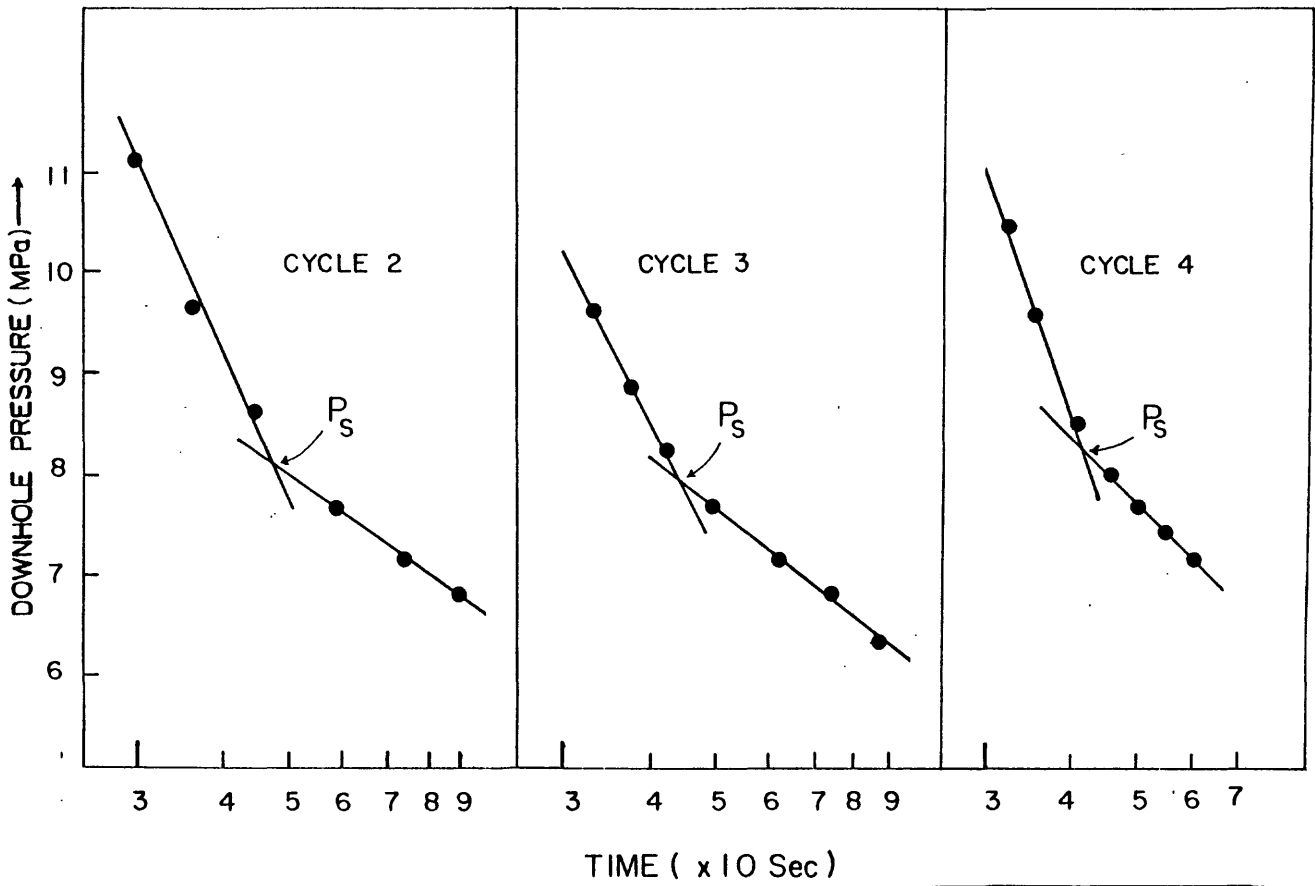


Fig. 5. Example showing the semilog method of choosing the ISIP. After Haimson and Lee (1984).

Nonlinear Regression Method. The nonlinear regression method is based on the observation of Muskat (1937) that as fluid flows between a well and porous rock, the pressure decays in a negative exponential fashion. The first segment of the curve immediately following shut in usually does not fit the exponential model because the fracture is still open. Assuming that the fracture loses its permeability after it closes, fluid flow into the well will be through the porous rock and will follow an exponential decay function of the form:  $P = a + \exp(b-ct)$  where  $a$ ,  $b$ , and  $c$  are constants,  $P$  is the borehole pressure, and  $t$  is time.

A nonlinear regression is run on the digitized pressure-time record from the time the well is shut in. If this regression does not provide a good fit to a negative exponential function, the first point is thrown out and the regression is run on the remaining points. This step is repeated until a negative exponential fit is achieved. The exponential curve is then extrapolated back to the point where shut in was initiated and that pressure is taken as the ISIP. An example of this method is shown in fig. 6.

Flow Rate vs Pressure Method. On cycles subsequent to the breakdown cycle, the pumping pressure at a constant flow rate usually stabilizes. These pumping pressures are most stable when the fracture is barely open. By plotting the various flow rates against the stable pumping pressures, the ISIP can be determined. When the fracture is closed, or nearly so, plotted points fit a steep straight line curve. When the fracture is open, the line has a shallower slope. The pressure at which the slope changes is taken to be the ISIP (fig. 7). This method works best when all the data are taken from a single cycle. This is because the fracture's behavior may change as it is extended away from the well bore.

Low Flow Rate Pumping. While pumping at a very low flow rate, the pressure usually increases until it reaches a stable pressure plateau. This pressure is the pressure at which the fracture is barely open, allowing fluid to leave the borehole at the same rate that it is being pumped in. The low flow rate pumping pressure is an upper bound on the ISIP.

## RESULTS

The seven intervals tested at Xiaguan were chosen by inspection of the core and televiewer logs. After fracturing, a rubber impression was taken of the test interval in order to determine the orientation of the induced fractures. The interval length was 2.5 m. General data on the borehole is presented in Table 1. A cycle by cycle tabulation of the results of each test is provided in the Appendix. Blank spaces on these tables mean that either the method was not attempted on that cycle or it did not work. By comparing the results of each method and inspecting the pressure records, upper and lower bounds were placed on the minimum and maximum horizontal stresses. These bounds, along with

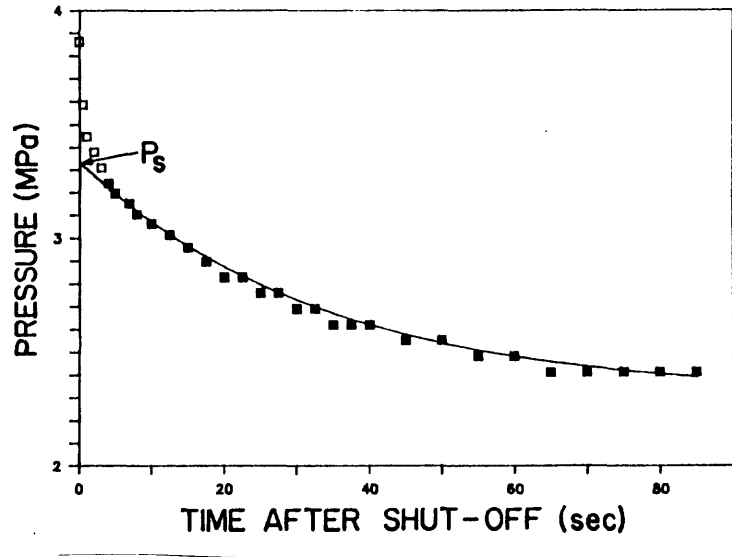


Fig. 6. Example of the negative exponential nonlinear regression method for choosing the ISIP (after Haimson and Lee, 1987).

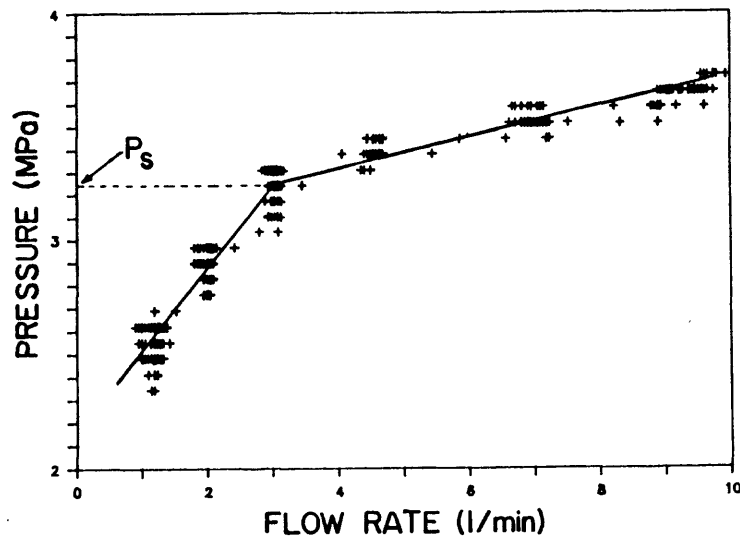


Fig. 7. Example of the flow-rate vs pressure method for choosing the ISIP (after Haimson and Lee, 1987).

TABLE 1

## General Data on the Xiaguan Borehole

Hole Name	Latitude and Longitude	Elevation (meters)	Water Level (meters)	Average Density
Xiaguan	25° 29'30"N 100° 19'48"E	2100	4	2.65

the vertical stress calculated from average densities, are provided in Table 2.

Test A - 85 m. The pressure rolled over rather than having a sharp peak on the initial cycles, indicating that there probably was not a breakdown. The televiewer shows four low-angle fractures, however a vertical fracture oriented N32E was found on the post-frac impression (fig.8), suggesting that a fracture may have been created. The interval was highly permeable, resulting in a rapid pressure drop to zero (surface pressure) after shut in. A range for  $S_{hmin}$  of 2.0 to 2.8 MPa is given, based on the range of best picks from the inflection point, low flow rate pumping pressure, flow rate vs pressure, and nonlinear regression methods. The semilog method did not work. The possible values of  $P_r$  range from 2.3 to 2.7 MPa, yielding an uncertainty of 36% in the value of  $S_{Hmax}$ .

TABLE 2

## Stress Determinations from Xiaguan

Test	Depth (m)	$S_{hmin}$ (MPa)		$S_{Hmax}$ (MPa)		$S_v$	Azimuth
		Min.	Max.	Min.	Max.		
A	85	2.0	2.8	2.5	5.3	2.3	N32E
B	198	7.8	8.5	13.9	17.2	5.2	N34E
C	214	7.5	8.6	10.8	15.6	5.7	N25E
D	233	5.2	6.0	7.3	10.9	6.2	N21E
E	250.5	6.7	7.4	11.7	14.3	6.6	Unknown
F	419	11.5	11.8	19.7	22.0	11.1	N2W
G	451.7	14.4	16.4	21.9	29.1	12.0	N7E

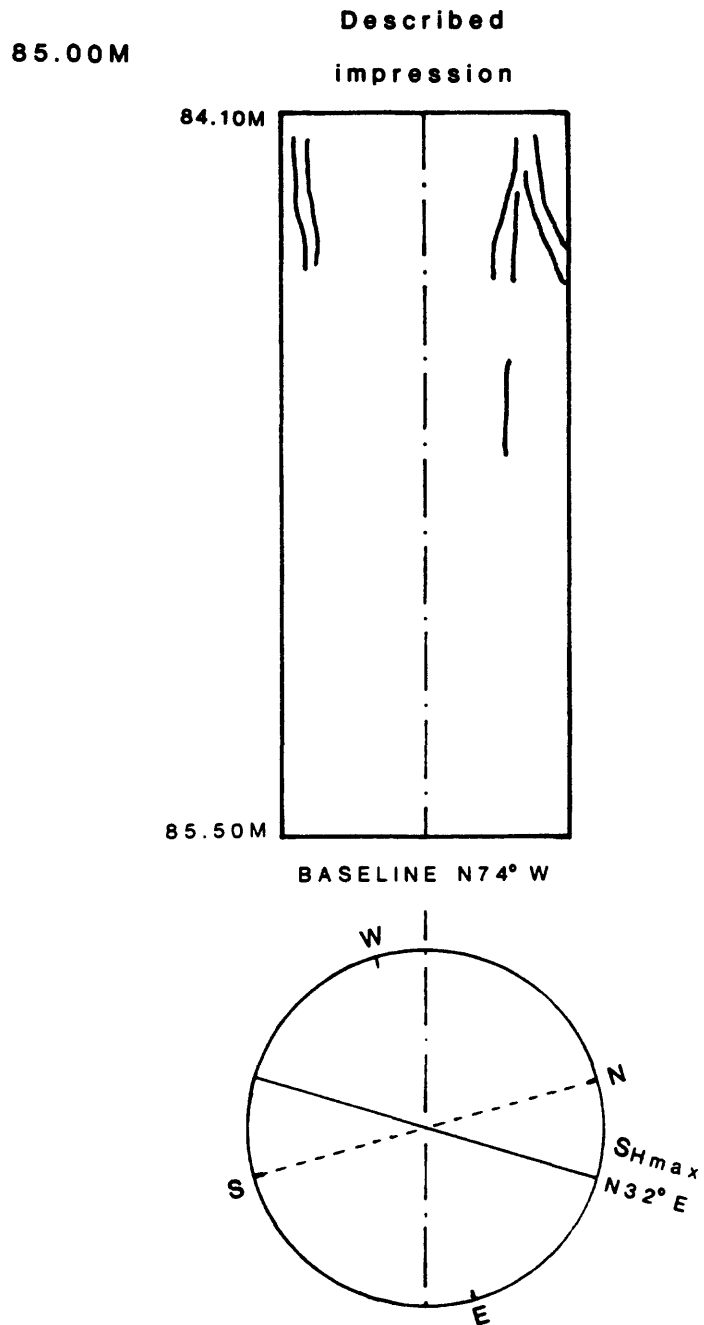


Fig. 8. Tracing of the impression packer from Test A.

Test B - 198 m. As in test A, there was no identifiable breakdown, although the impression revealed a high-angle fracture striking N34E not found on the televiewer log (fig. 9). The inflection point and nonlinear regression methods yielded values of 7.8 MPa and the flow rate vs pumping pressure yielded a slightly higher value of 8.5 MPa. Fracture reopening pressures from cycles 2, 3, and 4 yielded a value of 15.5 MPa (+ 10 %) for SHmax.

Test C - 214 m. A clear breakdown pressure of 10.9 MPa was achieved on the first cycle. The impression showed vertical fracture oriented N25E that had not been seen on the televiewer log (fig. 10). The decay curves showed clear inflection points, giving greater confidence to the estimate of Shmin. The inflection point method yielded an ISIP of 8.6 MPa on the 5th and 6th cycles, which is intermediate in value between those of the other methods. Nonlinear regression yielded an ISIP of 7.5 MPa. The semilog method yielded an anomalously low value of 6.8 MPa. The low flow-rate and flow-rate vs pressure methods gave values that were judged to be unusually high. The bounds for Shmin were taken as 7.5 to 8.6 MPa.

The fracture reopening pressures from cycles 2 and 3 were 9.6 and 8.1 MPa, respectively. This yields an uncertainty of 18 % for the value of SHmax.

Test D - 233 m. There was no distinguishable breakdown, although the impression revealed a vertical, N21E-striking fracture that was not visible on the televiewer log (fig. 11). The pressure decayed rapidly to zero after shut in on each cycle, reflecting the high permeability of the interval. The inflection point and nonlinear regression methods again yielded the most consistent results, although the inflection point values increased with later cycles. The semilog and flow-rate vs pressure methods yielded unusually low values for the ISIP. The low flow-rate pumping pressure was 6.0 MPa on both the second and third cycles and this was judged to be a good upper bound for Shmin. Fracture reopening pressures on cycles 2, 3, 4, 5, and 6 yielded a range from 4.8 to 6.0 MPa, giving an uncertainty of + 20 % to the value of SHmax.

Test E - 250 m. No breakdown was distinguishable on either of the first two cycles. Again, there was a vertical fracture on the impression that was not visible on the pre-fracturing televiewer log (fig. 12). Unfortunately, the orienting mark on the impression packer had been accidentally rotated and reconstruction of the orientation of the fracture is uncertain.

After shut-in, the pressures decayed rapidly to zero, although not as rapidly as in previous tests. The ISIP values obtained from the inflection point method varied considerably from cycle to cycle, as did the values from the nonlinear regression method. Representative ISIP values of 6.7 and 7.3 MPa were chosen from the inflection point and nonlinear regression

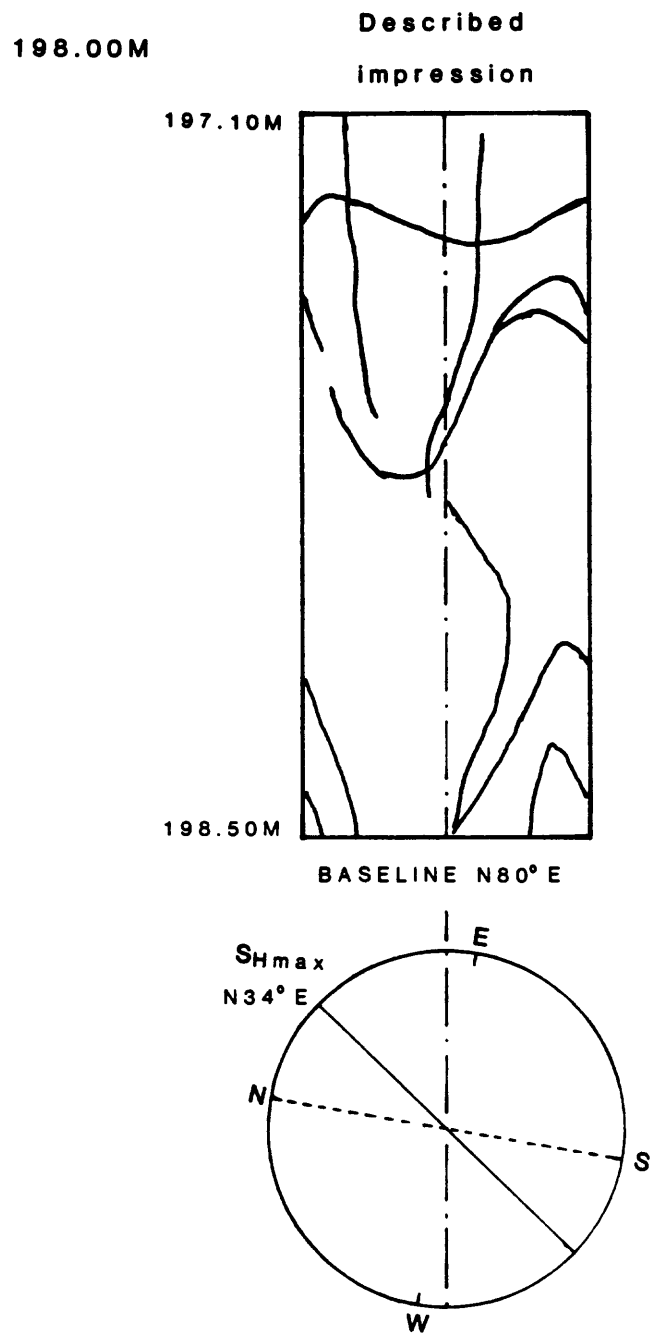


Fig. 9. Tracing of the impression packer from Test B.

214.00M Described  
impression

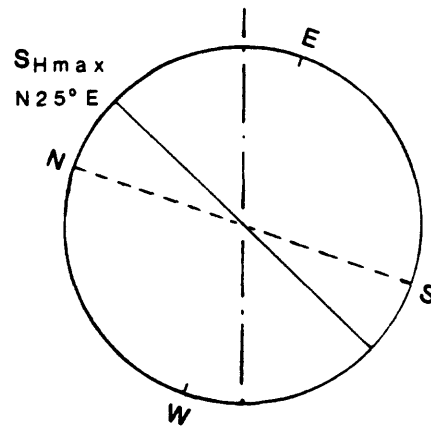
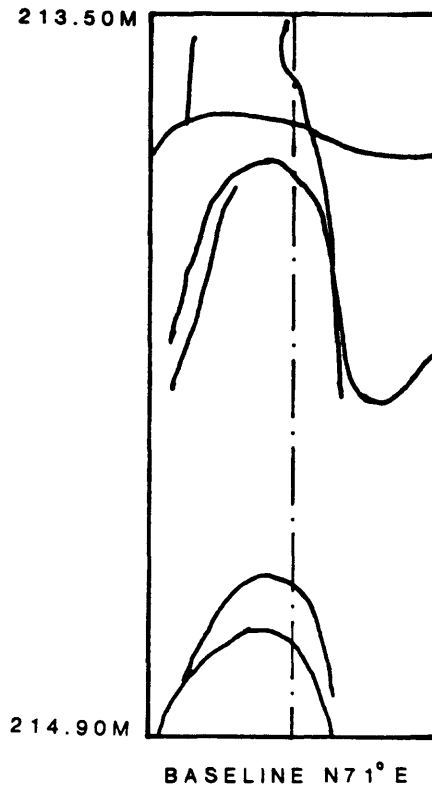


Fig. 10. Tracing of the impression packer from Test C.

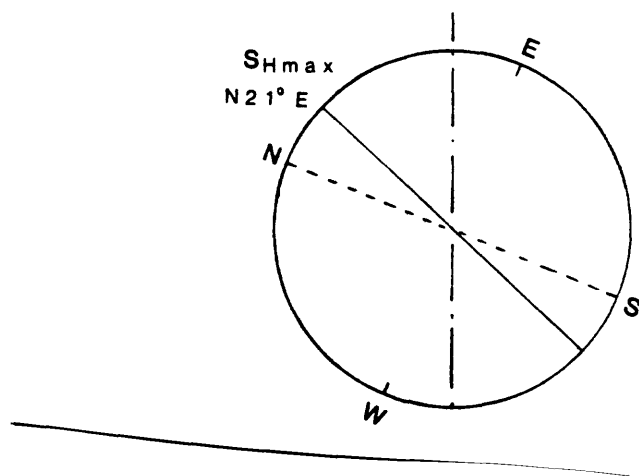
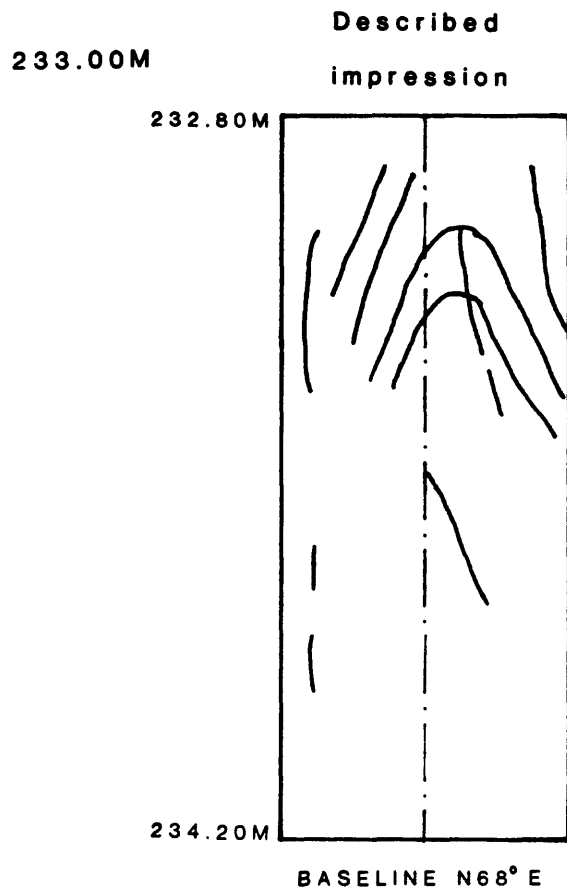


Fig. 11. Tracing of the impression packer from Test D.

250.50M Described impression

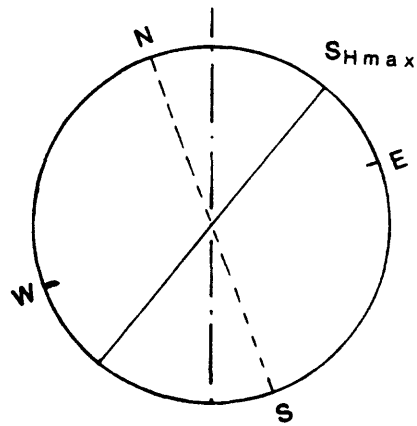


Fig. 12. Tracing of the impression packer from Test E.

methods, respectively. The low flow-rate pumping pressure of 7.4MPa gives a reasonable upper bound for  $Sh_{min}$ . The semilog and flow-rate vs pressure methods yielded values that were judged to be too low. The fracture reopening pressures, varied from 5.4 to 5.9 MPa on cycles 2, 4, 5, 6, 7, and 8 and resulted in an uncertainty of  $\pm 10\%$  for  $SH_{max}$ .

Test F - 419 m. No breakdown was seen on either of the first two cycles. A vertical fracture, not previously visible on the televiewer, was seen on the impression (fig. 13). It had an orientation of N2W. Pressure decay on the first two cycles was not too rapid, but became so on later cycles. Nevertheless, consistent ISIP values were picked by the inflection point method. These values showed a general decrease from one cycle to the next and an average value of 11.5 MPa was chosen as the best pick. The nonlinear regression method also worked fairly well, and the highest value of 11.8 MPa was chosen. The flow-rate vs pressure method gave an inconsistent set of points, and the resulting ISIP value was judged to be too tentative.

Test G - 452 m. The pumping rate on the first cycle was not sufficient to cause a breakdown, however, a clear breakdown of 24.0 MPa occurred on the second cycle. A previously unseen vertical fracture oriented N7E was revealed on the post-fracturing impression (fig. 14). ISIP values from the inflection point and nonlinear regression methods showed a general decrease from one cycle to the next. Values of 16.4 and 14.4 MPa were chosen from these two methods. The low flow-rate pumping pressure of 17.5 MPa provides a reasonable upper bound for  $Sh_{min}$ . The semilog method yielded a value that was judged to be too low and the flow-rate vs pressure method yielded a value that was judged to be too high.

## DISCUSSION

The rock in the Xiaguan well was highly fractured (Springer et al., 1987a) and each test interval had some inclined fractures visible on the televiewer log. The pressure-time records indicated clear breakdown pressures on only two of the seven tests, and rapid pressure decays after shut in suggested that the data were dominated by the presence of pre-existing fractures. The post-fracturing impressions, however, revealed vertical to subvertical fractures that were not visible on the televiewer record. The orientations yield a maximum horizontal stress direction of N20E + 13 deg, coinciding with the regional stress field inferred from faulting (Springer et al., 1987b). This provides strong evidence that real hydrofracs were created during these tests.

In general, the most consistent ISIP values were obtained from the inflection point and nonlinear regression methods. The flow-rate vs pressure method gave somewhat erratic results. The low flow-rate pumping pressures usually yielded the highest reasonable values, making them a reasonable upper bound in most cases. The semilog method only yielded a result in cases where

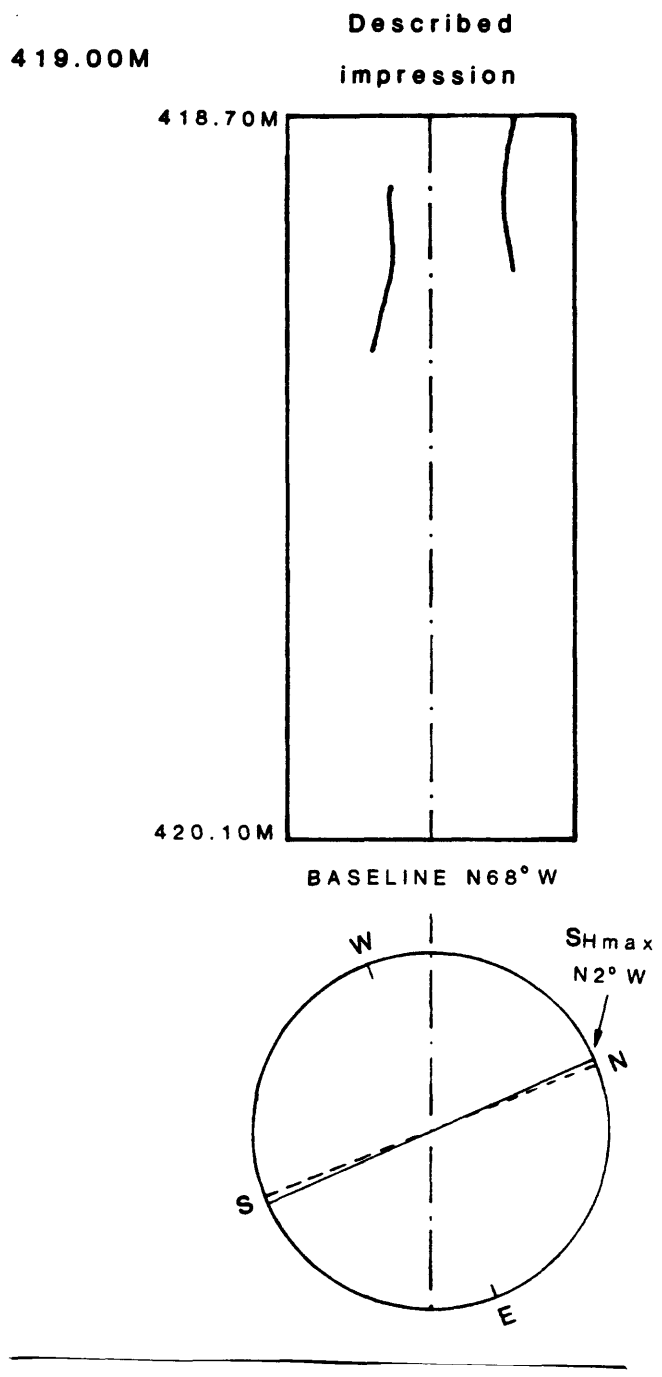


Fig. 13. Tracing of the impression packer from Test F.

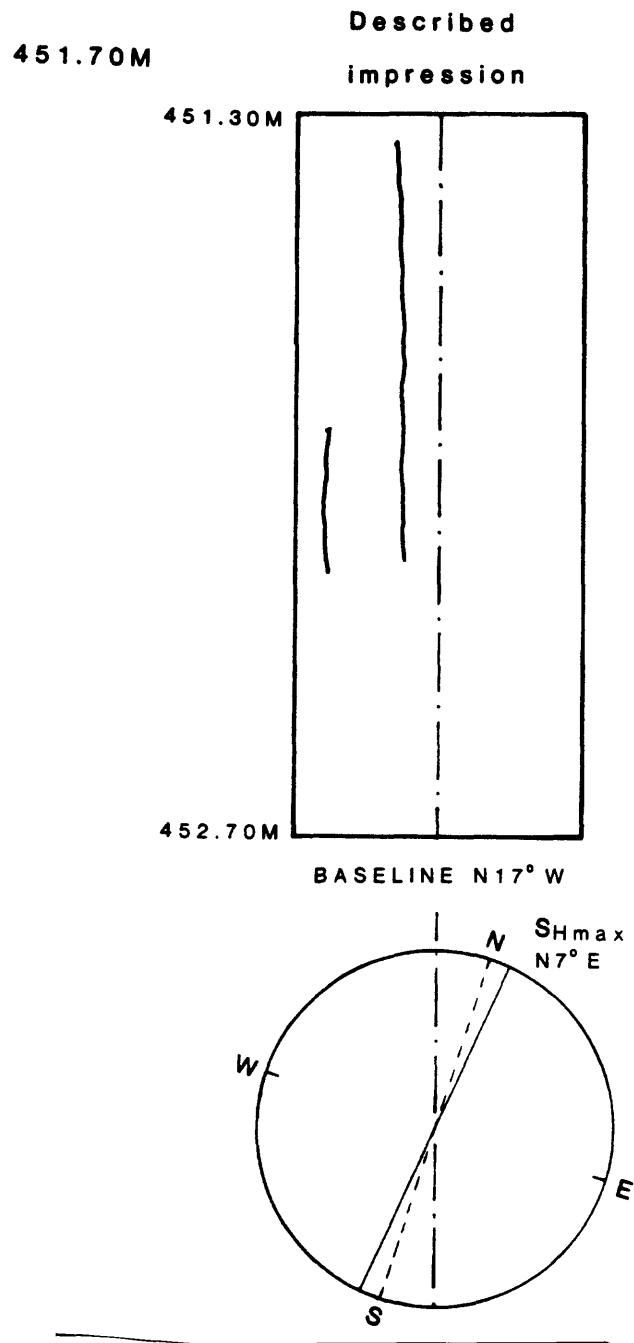


Fig. 14. Tracing of the impression packer from Test G.

other methods also worked. In each of these cases, the semilog method gave a value that was judged to be too low.

The values of  $S_{hmin}$  derived from the Xiaguan data are close to, and sometimes slightly higher than the lithostat as shown in fig. 15. Using the observation of Byerlee (1978) that, for normal stresses greater than 5 MPa, the coefficient of friction for most rocks is between 0.6 and 1.0, an envelope of failure on favorably oriented thrust faults was constructed (fig. 15) using the relationship derived by Zoback and Healy (1984):

$$S1-Po/S3-Po = [(\mu + 1)^2 + \mu^2]^{1/2} \quad [3]$$

where  $S1$  and  $S3$  are the maximum and minimum principal stresses, respectively and  $\mu$  is the coefficient of friction. The values of  $S_{Hmax}$  that fall in the failure envelope are from the tests at 214 m and 452 m. In both cases, only the high end of the range of uncertainty fell in the failure envelope. In the test at 214 m, the confining stresses are not much higher than 5 MPa so the conditions are close to the limit at which this method applies. The conclusion, therefore, is that the rocks are not close to failure in a thrust faulting mode at this site.

The stresses are transitional between a thrust and strike-slip faulting stress regime, that is  $S_{Hmax} > S_{hmin} > S_v$ , in the Xiaguan well. This is slightly higher than the strike-slip to normal stress regime implied by the seismicity and tectonics of the region (see Allen, 1984; Kan et al., 1977). High horizontal stresses at shallow depths, in regions of strike-slip faulting have been reported elsewhere (see Zoback et al., 1980). This may be caused by a decoupling of the shallow stress field from the deeper stresses related to earthquakes and faulting. The high relief in the area may also affect the shallow stress field and be responsible for the high stresses.

An older thrust fault intersected the well at 485 m as older ultramafic rocks were encountered above younger sediments (Springer et al., 1987a). An alternative explanation for the high horizontal stresses is that they are residual from a past thrusting event.

#### CONCLUSIONS

Five methods were used to determine the ISIP in the Xiaguan borehole. The inflection point, low flow-rate pumping pressure, flow-rate vs pressure, semilog, and nonlinear regression methods were used. Although the inflection point method is the most subjective of all methods, the end results from it were very consistent. The nonlinear regression method also yielded very good results. The low flow-rate pumping pressures provided a consistent upper bound for  $S_{hmin}$  as would be expected. Plotting pressure vs flow-rate provided fairly consistent results, although they were on the high side.

The semilog method was the least successful of all. It only

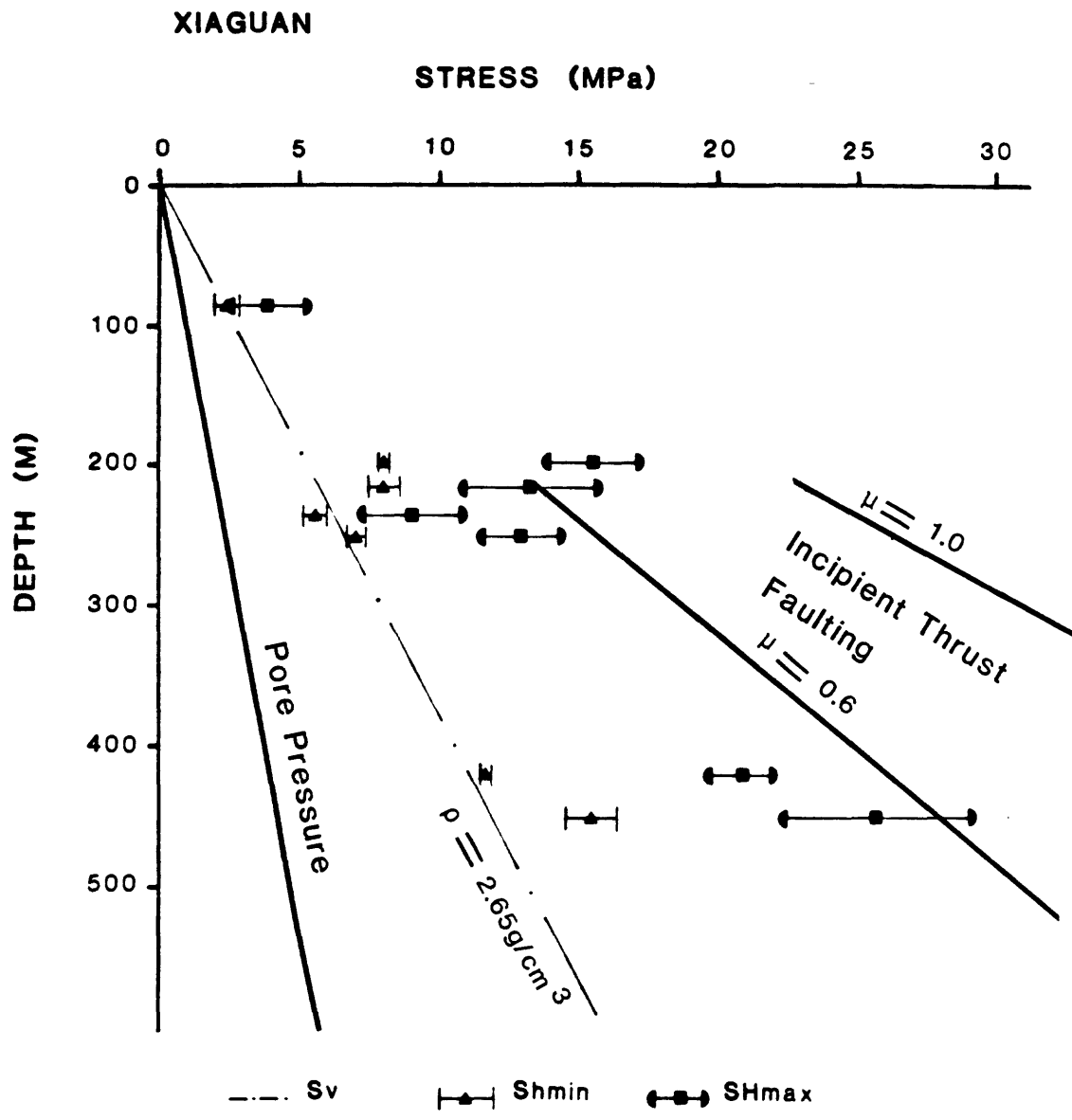


Fig. 15. Plot of  $S_{hmin}$ ,  $S_{Hmax}$ ,  $S_v$ , and  $P_o$  vs depth. The envelope of frictional failure in a thrust faulting mode is shown for frictional coefficient values of 0.6 to 1.0 using the relationship derived by Zoback and Healy (1984).

yielded an interpretable result in cases where the other methods worked well. The semilog results were consistently so much lower than the other methods that it was not judged to be a good lower bound on Shmin.

Clear breakdown pressures were not always seen on the pressure record. In the Xiaguan well, it may have been the result of nearly zero tensile strength of the rock. The main evidence for this is that in every test at Xiaguan, the impressions revealed high-angle fractures that were not visible on the pre-fracturing televiwer log.

Because the flow rates were so difficult to control, we had to estimate the fracture reopening pressures as large ranges of possible values. This was a problem in both holes and it resulted in uncertainties of up to 36% for the value of the maximum horizontal stress.

The measured values of Shmin were equal to or slightly higher than the theoretically calculated lithostat, indicating a transitional thrust to strike-slip stress regime. Calculation of the frictional stability of favorably oriented thrust faults suggests that the rocks are not close to failure in a thrust mode. Therefore, the measured stresses do not disagree with the observed normal to strike-slip tectonics of the region. The orientations of the hydraulic fractures were consistent and revealed a maximum horizontal stress orientation of N2W to N34E. This is in general agreement with the sense of horizontal slip on major faults in the region (Springer et al., 1987b).

#### REFERENCES

- Aamodt, R.L. and M. Kuriagawa, 1983, Measurement of instantaneous shut in pressure in Crystalline rock: in, Zoback, M.D. and B.C. Haimson, convenors, Hydraulic Fracturing Stress Measurements, National Academy Press, pp.139-142.
- Allen, C.R., Gillespie, A.R., Han Yuan, Sieh, K.E., Zhang Buchun, and Zhu Chengnan, 1984, Red River and associated faults, Yunnan Province, China: Quaternary geology, slip rates, and seismic hazard: Geological Society of America Bulletin, v.95, pp.686-700.
- Bredehoeft, J.D., R.G. Wolff, W.S. Keys, and E. Shuter, 1976, Hydraulic fracturing to determine the regional in-situ stress field, Piceance Basin, Colorado: Geological Society of America Bulletin, v.87, pp.250-258.
- Byerlee, J.D., 1978, Friction of rock: Pure and Applied Geophysics, v.116, pp.615-626.
- Gronseth, J.M. and P.R. Kry, 1983, Instantaneous shut-in pressure and its relationship to the minimum in-situ stress: in, Zoback, M.D. and B.C. Haimson, convenors, Hydraulic Fracturing Stress Measurements, National Academy Press, pp.55-60.
- Haimson, B.C. and M.Y. Lee, 1984, Development of wireline hydrofracturing and its use at the Monticello Reservoir, Final report to USGS Contract 14-08-0001-20537, 67p.

- Haimson, B.C. and M.Y. Lee, 1987, The state of stress and natural fractures in jointed preCambrian rhyolite in south-central Wisconsin: in, I.W. Farmer, J.J.K Daemen, C.S. Desai, C.E. Glass and S.P. Neuman, eds., Rock Mechanics, Proceedings of the 28th U.S. Symposium, pp.231-240.
- Haimson, B.C. and C. Fairhurst, 1967, Initiation and extension of hydraulic fractures in rock: Society of Petroleum Engineers Journal, v.7, pp.310-318.
- Haimson, B.C. and C. Fairhurst, 1970, In-situ stress determination at great depth by means of hydraulic fracturing: Proceedings, 11th U.S. Symposium on Rock Mechanics, American Society of Civil Engineers, pp.135-156.
- Hickman, S.H. and M.D. Zoback, 1983, The interpretation of hydraulic fracturing pressure-time data for in-situ stress determination: in, Zoback, M.D. and B.C. Haimson, convenors, Hydraulic Fracturing Stress Measurements, National Academy Press, pp.44-54.
- Hubbert, M.K. and D.G. Willis, 1957, Mechanics of hydraulic fracturing: Journal of Petroleum Technology, v.9, pp.153-168.
- Jaeger, J.C. and N.G.W. Cook, 1976, Fundamentals of Rock Mechanics: (2nd edition), Chapman Hall, John Wiley & Sons, New York.
- Kan Rongju, Zhang Sichang, Yan Fengtong, and Yu Linsheng, 1977, Present tectonic stress field and its relation to the characteristics of recent tectonic activity in southwest China: (in Chinese) Acta Geophysica Sinica, v.20, pp.96-109.
- Li Xianggen, Ran Yongkang, Peng Gui, Zhang Jing, Guo Shunmin, Xiang Hongfa, Chen Tieniu, Zhang Guowei, Ji, Fengju, and Ye Yongying, 1986, Active faults and their relationship with seismic activities in Dali of Yunnan Province and its adjacent regions: (in Chinese) Seismology and Geology, v. 8, no.4, pp.51-61.
- Liu Guangxun, Li Fangquan, and Li Guirong, 1986, Active tectonics and the state of stress in seismic region of northwest Yunnan Province, China: Seismology and Geology, v.8, no.1, 14p.
- McGarr A. and N.C. Gay, 1978, State of stress in the earth's crust: Annual Reviews of Earth and Planetary Science, v.6, pp.405-436.
- Muskat, M., 1937, Use of data on build-up of bottom-hole pressures: Transactions, American Institute of Mining and Metallurgical Engineers, v.123, pp.44-48.
- Springer, J.E., Zhai Qingshan, M.D. Zoback, and Li Fangquan, 1987a, Analysis of fractures from televiwer logs of a 500 m-deep well at Xiaguan, Yunnan Province, China: U.S. Geological Survey, open-file report, 87-432, 30p.
- Springer, J.E., Zhai Qingshan, and Svitek, J.F., 1987b, Summary of the geologic setting and televiwer logs from the Yongping test well, Yunnan Province, China: U.S. Geological Survey, Open-file Report, 87-427, 28p.
- Wu Daning and Deng Qidong, 1985, Primary behavior of northwest Yunnan: Tectonic subsidence area and mechanics: (in Chinese) Modern Crustal Movement Research, v.1, pp.118-132.
- Yan Shihua, Huang Kun, and Zhang Zusheng, 1983, Analysis of the

horizontal deformation in Xiaguan-Weishan, Yunnan Province:  
(in Chinese) Journal of Seismological Research, v.6, pp.477-486.

- Zoback, M.D., H. Tsukahara, and S.H. Hickman, 1980, Stress measurements at depth in the vicinity of the San Andreas fault; implications for the magnitude of shear stress at depth: Journal of Geophysical Research, v.85, pp.6157-6173.
- Zoback, M.D. and J.H. Healy, 1984, Friction, faulting, and in-situ stress: Annales Geophysicae, v.2, pp.689-698.
- Zoback, M.L. and M.D. Zoback, 1980, State of stress in the conterminous United States: Journal of Geophysical Research, v.85, pp.6113-6156.

APPENDIX

Cycle by Cycle Results of the Hydrofracturing Tests

TABLE A1  
ISIP Determinations from Xiaguan  
(Downhole Pressures in MPa)

Cycle	IP	LF	SL	NLR
<b>Test A: Depth = 85 m Po = 0.8 MPa FR result = 2.8 MPa</b>				
1	2.5	--	--	2.8
2	2.0	--	--	--
3	2.0	--	--	2.1
4	2.0	2.3	--	--
5	2.8	--	--	--
6	--	--	--	--
7	2.8	--	--	--
8	2.9	--	--	--
Best Pick:	2.0	2.3	--	2.8
<b>Test B: Depth = 198 m Po = 1.9 MPa FR result = 8.5 MPa</b>				
1	--	--	--	5.6
2	7.8	--	--	7.8
3	6.6	--	--	6.0
4	--	--	--	--
5	--	--	--	--
Best Pick:	7.8	--	--	7.8
<b>Test C: Depth = 214 m Po = 2.1 MPa FR result = 9.4 (3rd cycle)</b>				
1	--	--	7.1	7.0
2	9.1	--	--	6.5
3	--	9.0	6.4	8.5
4	8.7	--	7.0	7.8
5	8.6	--	--	--
6	8.6	--	--	--
Best Pick:	8.6	9.0	6.8 (ave)	7.5 (ave)
<b>Test D: Depth = 233 m Po = 2.3 MPa FR result = 4.5 MPa</b>				
1	6.0	--	3.0?	6.5
2	5.2	6.0	2.6?	4.1
3	5.2	6.0	2.4?	5.4
4	6.3	--	--	--
5	5.7	--	2.4?	--
6	5.7	--	2.5?	--
Best Pick:	5.2	6.0	2.6 (ave)	5.3 (ave)

Methods: IP=Inflection Point, LF=Low Flow-Rate Pumping Pressure, SL=Semilog Method, NLR=Nonlinear Regression, FR=Flow-Rate vs Pressure.

TABLE 1A (continued)  
 ISIP Determinations from Xiaguan  
 (Downhole Pressures in MPa)

Cycle	IP	Method LF	SL	NLR
<b>Test E:    Depth = 250.5 m,    Po = 2.5 MPa, FR result = 5.3 MPa</b>				
1	8.4	--	4.6?	8.8
2	7.6	--	4.0?	7.3
3	5.9	--	--	7.8
4	6.7	--	--	--
5	7.3	7.4	3.9?	--
6	9.4	--	4.3?	--
7	6.9	7.2	--	--
8	7.6	--	4.9?	--
Best Pick:	6.7	7.4	4.3?	7.3
<b>Test F:    Depth = 419 m    Po = 4.1 MPa    FR result = 11.3 MPa</b>				
1	11.1	--	--	11.4
2	11.9	--	--	10.7
3	11.7	--	--	10.0
4	11.5	--	--	11.8
5	12.2	--	--	11.5
6	11.7	--	--	--
7	10.2	--	--	--
Best Pick:	11.5(ave)	--	--	11.8
<b>Test G:    Depth = 452 m    Po = 4.4 MPa    FR result = 18.6 MPa</b>				
1	--	--	--	18.3?
2	--	--	--	13.8
3	20.6	--	15.3	14.4
4	16.7	17.5	13.5	--
5	16.4	--	13.3	--
6	15.9	--	14.0	--
7	16.4	--	14.8	--
Best Pick:	16.4	17.5	14.2(ave)	14.4

TABLE 2A  
Breakdown and Fracture Reopening Pressures from Xiaguan  
(Downhole Pressures in MPa)

Test	Cycle	Pb	Pr
A		--	
85 m	2		2.7
	3		2.3
	4		2.0
Picks:		no breakdown	2.3 to 2.7
B		--	
198 m	2		7.6
	3		7.3
	4		6.4
Picks:		no breakdown	6.4 to 7.6
C		10.9	--
214 m	2		9.6
	3		8.1
Picks:		10.9	8.1 to 9.6
D		--	--
233 m	2		5.2
	3		4.8
	5		6.0
	6		5.2
Picks:		no breakdown	4.8 to 6
E		--	--
250.5 m	2		5.9
	4		5.9
	5		5.7
	6		7.6
	7		5.4
	8		5.9
Picks:		no breakdown	5.4 to 5.9
F		--	--
419 m	2		10.5
	3		9.0
	4		10.5
	5		10.2
	6		10.7
Picks:		no breakdown	9.0 to 10.7
G		24.0	--
451.7 m	4		16.9
	5		15.7
	6		16.1
	7		16.7
Picks:		24.0	15.7 to 16.9